Monthly Notices of the ROYAL ASTRONOMICAL SOCIETY

MNRAS **452,** 2930–2939 (2015) doi:10.1093/mnras/stv1478

How clustering dark energy affects matter perturbations

A. Mehrabi,[1★] S. Basilakos[2] and F. Pace[3]

[1]*Department of Physics, Bu-Ali Sina University, Hamedan 65178, Iran*
[2]*Academy of Athens, Research Center for Astronomy & Applied Mathematics, Soranou Efessiou 4, 11-527 Athens, Greece*
[3]*Jodrell Bank Centre for Astrophysics, School of Physics and Astronomy, The University of Manchester, Manchester M13 9PL, UK*

Accepted 2015 July 1. Received 2015 June 30; in original form 2015 April 6

ABSTRACT

The rate of structure formation in the Universe is different in homogeneous and clustered dark energy models. The degree of dark energy clustering depends on the magnitude of its effective sound speed $c^2_{\rm eff}$ and for $c^2_{\rm eff}=0$ dark energy clusters in a similar fashion to dark matter while for $c^2_{\rm eff}=1$ it stays (approximately) homogeneous. In this paper we consider two distinct equations of state for the dark energy component, $w_{\rm d}=$ const and $w_{\rm d}=w_0+w_1\left(\frac{z}{1+z}\right)$ with $c^2_{\rm eff}$ as a free parameter and we try to constrain the dark energy effective sound speed using current available data including Type Ia supernovae, baryon acoustic oscillation, cosmic microwave background shift parameter (*Planck* and *WMAP*), Hubble parameter, big bang nucleosynthesis and the growth rate of structures $f\sigma_8(z)$. At first we derive the most general form of the equations governing dark matter and dark energy clustering under the assumption that $c^2_{\rm eff}=$ const. Finally, performing an overall likelihood analysis we find that the likelihood function peaks at $c^2_{\rm eff}=0$; however, the dark energy sound speed is degenerate with respect to the cosmological parameters, namely $\Omega_{\rm m}$ and $w_{\rm d}$.

Key words: Methods: analytical – cosmological parameters – cosmology: theory – dark energy.

1 INTRODUCTION

We are living in a special epoch of the cosmic history where the expansion of the Universe is accelerated due to an unknown energy component, usually dubbed dark energy (DE). This acceleration has been discovered observationally using the luminosity distance of Type Ia supernovae (SnIa; Perlmutter et al. 1997, 1998, 1999; Riess et al. 2004; Astier et al. 2006; Jha, Riess & Kirshner 2007). In addition to this, other observations including the cosmic microwave background (CMB; Bennett et al. 2003; Spergel et al. 2003, 2007; Planck Collaboration XIII 2015; Planck Collaboration XIV 2015), large-scale structures (LSS; Hawkins et al. 2003; Tegmark et al. 2004; Cole et al. 2005) and baryon acoustic oscillation (BAO; Eisenstein et al. 2005; Seo & Eisenstein 2005; Blake et al. 2011) support an accelerated expansion. At a fundamental level there are two different approaches to describe the phenomenon of the cosmic acceleration and indeed many efforts are devoted to investigate its deep nature both observationally and theoretically. One way is to consider a fluid with a sufficiently negative pressure dubbed DE and the other is based on the modification of the laws of gravity on large scales. The first approach comes in many different scenarios. The simplest one is a very tiny cosmological constant Λ in Einstein field equations that has a (negative) pressure equal to its energy density and equation-of-state (EoS) parameter $w_{\rm d}=\frac{p_{\rm d}}{\rho_{\rm d}}=-1$ (Weinberg 1989; Sahni & Starobinsky 2000; Peebles & Ratra 2003). The overall theoretical cosmological model (cosmological constant plus cold dark matter to explain galaxy rotation curves and the potential well for structure formation) is called ΛCDM model. Despite being highly consistent with observational data, the ΛCDM model suffers of two theoretical problems, namely the fine-tuning and the cosmic coincidence problem (Weinberg 1989; Sahni & Starobinsky 2000; Peebles & Ratra 2003). Differently from the cosmological constant case with EoS $w_{\rm d}=-1$, other dynamical models have been largely studied in the literature and usually categorized in two branches, quintessence models (Armendariz-Picon, Mukhanov & Steinhardt 2000; Copeland, Sami & Tsujikawa 2006) and *k*-essence models (Armendariz-Picon, Damour & Mukhanov 1999; Armendariz-Picon et al. 2000; Chiba, Okabe & Yamaguchi 2000; Chiba, Dutta & Scherrer 2009; Amendola & Tsujikawa 2010).

The simplest way to modify gravity is to consider Einstein–Hilbert Lagrangian as a generic function of the Ricci scalar R ($f(R)$ theories; Schmidt 1990; Magnano & Sokolowski 1994; Dobado & Maroto 1995; Capozziello, Carloni & Troisi 2003; Carroll et al. 2004) or add extra-dimension models like in the DGP model (Dvali, Gabadadze & Porrati 2000). Understanding which class of models is the real one is one of the biggest challenges for cosmology.

In addition to the background evolution, LSS provide valuable information about the nature of DE (Tegmark et al. 2004, 2006). Primordial matter perturbations grow throughout the cosmic history

★ E-mail: mehrabi@basu.ac.ir

and their growth rate depends on the overall energy budget and on the properties of the cosmic fluids. DE slows down the growth rate of LSS. Structures grow due to gravitational instability and DE acts opposing and reducing the growth rate. The growth rate of structures can be measured from the redshift space distortion (RSD). Inward peculiar velocities of LSS generate a distortion that is directly related to the matter density contrast.

Since the cosmological constant does not change in space and time, it cannot cluster like dark matter (DM) and it has a negligible contribution to the energy density of the universe at high redshift. On the other hand, dynamical DE can cluster and the amount of clustering depends strongly on its effective sound speed. The effective sound speed is defined as $c_{\rm eff}^2 = c_{\rm e} = \frac{\delta p_{\rm d}}{\delta \rho_{\rm d}}$ (hereafter we use $c_{\rm e}$) where $\delta p_{\rm d}$ and $\delta \rho_{\rm d}$ are the pressure and energy density perturbations for DE, respectively, and coincides with the actual sound speed in the DE comoving rest frame (Hu 1998). In quintessence models we have $c_{\rm e} \simeq 1$ so DE perturbations cannot grow on sub-horizon scales while in *k*-essence models the effective sound speed can be tiny ($c_{\rm e} \ll 1$; Armendariz-Picon et al. 1999, 2000; Garriga & Mukhanov 1999; Babichev, Mukhanov & Vikman 2006; Akhoury, Garfinkle & Saotome 2011) and DE perturbations grow similarly to DM perturbations. The possibility of DE clustering has been studied by many authors (Erickson et al. 2002; Bean & Doré 2004; Hu & Scranton 2004; Ballesteros & Riotto 2008; de Putter, Huterer & Linder 2010; Sapone & Majerotto 2012; Batista & Pace 2013; Dossett & Ishak 2013; Basse et al. 2014; Batista 2014; Pace, Batista & Del Popolo 2014; Steigerwald, Bel & Marinoni 2014). In particular, it has been shown that the homogeneous DE scenario fails to reproduce the observed concentration parameter of the massive galaxy clusters (Basilakos, Bueno Sanchez & Perivolaropoulos 2009). In this framework, de Putter et al. (2010) pointed out that CMB and LSS slightly prefer dynamical DE with $c_{\rm e} \neq 1$ and recently Mehrabi, Malekjani & Pace (2015) and Basilakos (2015) have shown that clustering DE reproduces the growth data better in the framework of the spherical collapse model. A similar conclusion was suggested also by Nesseris & Sapone (2015).

The growth rate $f = \frac{d\ln\delta_{\rm m}}{d\ln a}$ is usually approximated by $f = \Omega_{\rm m}^{\gamma}$ as first introduced by Peebles (1993). In this parametrization γ is the so-called growth index and can be used to distinguish between DE and modified gravity models (Linder 2005; Huterer & Linder 2007; Basilakos & Pouri 2012; Rapetti et al. 2013). It is well known that for a ΛCDM model γ is independent of redshift and equal to 6/11. The evolution of the matter density $\Omega_{\rm m}$ depends on the evolution of the Hubble parameter $H(a)$ and hence on the particular cosmological model adopted. In this paper we consider two distinct models, a constant $w_{\rm d}$ and a dynamical $w_{\rm d}(z)$, and we consider $c_{\rm eff}$ as a free parameter. Then based on the linear regime we numerically solve the perturbed general relativity (GR) equations to evaluate the growth rate of matter in the presence of DE clustering. Using a Markov Chain Monte Carlo (MCMC) method we can constrain the cosmological parameters using SnIa, BAO, CMB shift parameter, the Hubble parameter, the big bang nucleosynthesis (BBN) and growth rate data $f\sigma_8(z)$.

The structure of this paper is as follows. In Section 2, we derive the equations governing the linear growth of matter perturbations in a general relativistic framework and show the effects of DE clustering on the growth rate of matter. In Section 3, we present all the details of the observational data used in this work to constrain the cosmological parameters including the DE sound speed and their uncertainties. In Section 4, we provide for the first time (to our knowledge) an approximated solution of the growth index of matter fluctuations as a function of the cosmological parameters, DE perturbations and $c_{\rm e}$. Finally in Section 5 we conclude and discuss our results.

2 EFFECT OF DE SOUND SPEED ON THE GROWTH RATE OF MATTER PERTURBATIONS

In this section we revise the fundamental equations necessary to our analysis. The sound horizon of DE with effective sound speed $c_{\rm e}$ in an Friedmann-Robertson-Walker (FRW) universe is given by

$$\lambda_{\rm s}(a) = \int_{a_{\rm i}}^{a} \frac{c_{\rm e}(x)}{x\mathcal{H}(x)} {\rm d}x, \tag{1}$$

where $\mathcal{H} = \frac{a'}{a}$, the prime being the derivative with respect to conformal time (η) and $a_{\rm i}$ an initial scale factor. The nominal Hubble parameter is given by $H = \frac{\dot{a}}{a}$ and thus $\mathcal{H} = aH$ which implies

$$\frac{\mathcal{H}'}{\mathcal{H}^2} = 1 + \frac{\dot{H}}{H^2}, \tag{2}$$

where an overdot refers to a derivative with respect to the cosmic time (t). In the case of $c_{\rm e} \simeq 1$, pressure suppresses any DE perturbation with the consequence that DE may cluster only on scales comparable to the horizon.

The opposite situation holds if $c_{\rm e} \ll 1$. Indeed in this case DE can cluster in analogy to the DM component and perturbations will grow with time. DE clustering modifies the evolution of DM perturbation and thus it affects the rate of structure formation in the universe.

We start our derivation of the relevant equations by considering the line element of an expanding universe in the Newtonian gauge without anisotropic stress:

$${\rm d}s^2 = -(1+2\phi){\rm d}t^2 + a^2(t)(1-2\phi){\rm d}\boldsymbol{x}^2, \tag{3}$$

where ϕ is the Bardeen potential. First-order Einstein equations in Fourier space are

$$3\mathcal{H}\phi' + \left(3\mathcal{H}^2 + k^2\right)\phi = -\frac{3\mathcal{H}^2}{2}(\Omega_{\rm m}\delta_{\rm m} + \Omega_{\rm d}\delta_{\rm d}), \tag{4}$$

$$\phi'' + 3\mathcal{H}\phi' + \left(\frac{2a''}{a} - \mathcal{H}^2\right)\phi = \frac{3\mathcal{H}^2}{2}\Omega_{\rm d}\frac{\delta p_{\rm d}}{\delta\rho_{\rm d}}\delta_{\rm d}, \tag{5}$$

where $\Omega_{\rm m} = \Omega_{\rm DM} + \Omega_{\rm b}$ ($\Omega_{\rm d} = 1 - \Omega_{\rm m}$) is the matter (DE) density parameter and $\delta_{\rm m}$ ($\delta_{\rm d}$) is the corresponding density contrast. The first-order energy-momentum conservation equations for a generic fluid with EoS parameter w are (Ma & Bertschinger 1995)

$$\delta' = -(1+w)(\theta - 3\phi') - 3\frac{a'}{a}\left(\frac{\delta p}{\delta\rho} - w\right)\delta, \tag{6}$$

$$\theta' = -\frac{a'}{a}(1-3w)\theta - \frac{w'}{1+w}\theta + \frac{\frac{\delta p}{\delta\rho}}{1+w}k^2\delta + k^2\phi. \tag{7}$$

These equations are correct for any fluid with $p = w\rho$ (for dust $w = 0$ and for DE $w = w_{\rm d}$), where δ is the density contrast, θ is the divergence of the fluid velocity ($\theta = {\rm i}k^i v_i$) and $\frac{\delta p}{\delta\rho}$ can be written as (Bean & Doré 2004)

$$\frac{\delta p}{\delta\rho} = c_{\rm e} + 3\mathcal{H}(1+w)(c_{\rm e} - c_{\rm ad}^2)\frac{\theta}{\delta}\frac{1}{k^2}, \tag{8}$$

where $c_{\rm ad}^2 = c_{\rm a}$ is the DE adiabatic sound speed

$$c_{\rm a} = w - \frac{w'}{3\mathcal{H}(1+w)}. \tag{9}$$

Note that the second term on the right-hand side of equation (8) appears because we demand pressure perturbations to be a gauge invariant quantity (Bean & Doré 2004). For a perfect fluid, perturbations in the pressure are purely determined by the adiabatic sound speed but for an imperfect fluid, dissipative processes generate entropic perturbations and therefore we have a more general relation. In this case, c_e acts like a proxy for pressure perturbations and the growth of perturbation in the DE component depends on the effective sound speed and not on the adiabatic sound speed any more. In the following this statement will be confirmed by solving the perturbed equations numerically.

To study the effect of the DE sound speed on structure formation, we consider a universe with pressure-less DM and a DE component with varying EoS that we specialize to $w_d(z) = w_0 + w_1 \frac{z}{1+z}$. The latter parametrization is the well-known Chevallier–Polarski–Linder (CPL) parametrization (Chevallier & Polarski 2001; Linder 2003). We eliminate θ from equations (6) and (7) and find two second-order differential equations for the density contrast of DM and DE. In addition using $\frac{d}{d\eta} = a\mathcal{H}\frac{d}{da}$ and $\frac{d^2}{d\eta^2} = a^2\mathcal{H}^2\frac{d^2}{da^2} + (a\mathcal{H}^2 + a\dot{\mathcal{H}})\frac{d}{da}$, these equations can be written in terms of the scale factor. Finally our desired equations governing the growth of DM and DE perturbations are

$$\frac{d^2\delta_m}{da^2} + A_m\frac{d\delta_m}{da} + B_m\delta_m = S_m, \tag{10}$$

$$\frac{d^2\delta_d}{da^2} + A_d\frac{d\delta_d}{da} + B_d\delta_d = S_d, \tag{11}$$

and the coefficients (see also equation 2) are

$$\begin{aligned}
A_m &= \frac{1}{a}\left(2 + \frac{\mathcal{H}'}{\mathcal{H}^2}\right) = \frac{1}{a}\left(3 + \frac{\dot{H}}{H^2}\right),\\
B_m &= 0,\\
S_m &= 3\frac{d^2\phi}{da^2} + \frac{3}{a}\left[2 + \frac{\mathcal{H}'}{\mathcal{H}^2}\right]\frac{d\phi}{da} - \frac{k^2}{a^2\mathcal{H}^2}\phi,\\
A_d &= \frac{1}{a}\left[2 + \frac{\mathcal{H}'}{\mathcal{H}^2} + 3c_a - 6w_d\right],\\
B_d &= \frac{1}{a^2}\left[3(c_e - w_d)\left(1 + \frac{\mathcal{H}'}{\mathcal{H}^2} - 3w_d + 3c_a - 3c_e\right)\right.\\
&\quad \left. + \frac{k^2}{\mathcal{H}^2}c_e - 3a\frac{dw_d}{da}\right],\\
S_d &= (1 + w_d)\left[3\frac{d^2\phi}{da^2} + \frac{3}{a}\left(2 + \frac{\mathcal{H}'}{\mathcal{H}^2} - 3c_a\right)\frac{d\phi}{da}\right.\\
&\quad \left. - \frac{k^2}{a^2\mathcal{H}^2}\phi + \frac{3}{1 + w_d}\frac{d\phi}{da}\frac{dw_d}{da}\right],
\end{aligned} \tag{12}$$

where $\frac{\mathcal{H}'}{\mathcal{H}^2}$ (or $\frac{\dot{H}}{H^2}$) is a function of the scale factor and using Friedmann equations we have

$$\frac{\mathcal{H}'}{\mathcal{H}^2} = -\frac{1}{2}\frac{\Omega_m + \Omega_d(1 + 3w_d)}{\Omega_m + \Omega_d} = -\frac{1}{2}(1 + 3\Omega_d w_d). \tag{13}$$

These equations are not in agreement with equation (44) in Abramo et al. (2009), which were obtained in the limit of a matter-dominated universe ($\frac{\mathcal{H}'}{\mathcal{H}^2} = -\frac{1}{2}$) and a constant w_d. To resolve this discrepancy, see Appendix A.

We integrate equations (10) and (11) numerically from $z_i = 100$ to $z = 0$, in order to obtain the density contrast of DM and DE. We use the same procedure of Abramo et al. (2009) to find the initial conditions. In the matter-dominated era $\phi' \simeq 0$, so from equation (4) we have

$$\delta_{m,i} = -2\phi_i\left(1 + \frac{k^2}{3\mathcal{H}_i{}^2}\right), \tag{14}$$

for the initial value of δ_m and

$$\frac{d\delta_{m,i}}{da} = -\frac{2}{3}\frac{k^2}{\mathcal{H}_i{}^2}\phi_i, \tag{15}$$

for its derivative. For δ_d the initial value is set using the adiabatic perturbations condition (Kodama & Sasaki 1984; Amendola & Tsujikawa 2010),

$$\delta_{d,i} = (1 + w_d)\delta_{m,i}, \tag{16}$$

and its derivative is set to

$$\frac{d\delta_{d,i}}{da} = (1 + w_d)\frac{d\delta_{m,i}}{da} + \frac{dw_d}{da}\delta_{m,i}. \tag{17}$$

According to the above argument, by fixing the initial condition of ϕ_i we have all the initial conditions. We set $\phi_i = -6 \times 10^{-7}$ which corresponds to $\delta_m = 0.1$ at present time for $k = 0.1\,h\,\mathrm{Mpc}^{-1}$. Our results are robust under small changes of the initial conditions, and we do not worry about the exact values. (For $\phi_i = -7 \times 10^{-8}$, δ_m reach to 0.01 at present time but $f\sigma_8$ differs less than 10^{-4} per cent.)

DE clustering affects the growth of matter perturbations through the change of the potential ϕ. As we noticed the amount of DE clustering is directly related to its effective sound speed. We restrict our analysis to the choice of $k = 1/\lambda = 0.1\,h\,\mathrm{Mpc}^{-1}$ which corresponds to $\lambda = 10\,h^{-1}\,\mathrm{Mpc}$ (Zhang et al. 2012). Note that the power-spectrum normalization σ_8 which is the rms mass fluctuation on a scale $R_8 = 8\,h^{-1}\,\mathrm{Mpc}$ corresponds to $k = 0.125\,h\,\mathrm{Mpc}^{-1}$. On the other hand it has been common practice to assume that the shape of the power spectrum recovered from galaxy surveys matches the linear matter power spectrum shape on scales $k \le 0.15\,h\,\mathrm{Mpc}^{-1}$ (Smith et al. 2003; Tegmark et al. 2004; Percival et al. 2007). Obviously the choice of $k = 0.1\,h\,\mathrm{Mpc}^{-1}$ assures that we are in the linear regime. We find that small variations around this value do not really affect the qualitative evolution of the growth rate of clustering and thus of $\gamma(z)$.[1]

To compare these results with observations we calculate the growth factor $f(z) = -\frac{1+z}{\delta_m(z)}\frac{d\delta_m(z)}{dz}$ and the growth index $\gamma(z) = \frac{d\ln f(z)}{d\Omega_m(z)}$ using our numerical results. The growth index in the ΛCDM model is redshift independent and approximately equal to $\gamma = 0.55$. To compare this model to observational data we need to evaluate $f(z)\sigma_8(z)$, where $\sigma_8(z)$ is the mass variance in a sphere of radius of 8 Mpc h^{-1}. The variance $\sigma_8(z)$ can be written in terms of σ_8 at present time as $\sigma_8(z) = \sigma_8(z=0)\frac{\delta_m(z)}{\delta_m(z=0)}$. Also, in order to treat $\sigma_8 \equiv \sigma_8(z=0)$ properly for the DE models we rescale the value of σ_8 by $\sigma_8 = \frac{\delta_m(z=0)}{\delta_{m,\Lambda}(z=0)}\sigma_{8,\Lambda}$. Regarding $\sigma_{8,\Lambda}$ we utilize $\sigma_{8,\Lambda} = 0.818(0.30/\Omega_m)^{0.26}$ provided by the *Planck* analysis of Spergel, Flauger & Hložek (2015) and it is also in agreement with the results of *Planck* 2015 (Planck Collaboration XIII 2015).

DE perturbations not only depend on the sound speed but also on the EoS w_d. In the limit $w_d \to -1$ all DE perturbations are washed out due to the $1 + w_d$ factor in front of the source term in the evolution equation of δ_d. To show how the DE sound speed affects the linear evolution of DM, we consider $\Omega_m = 0.28$ and $h = 0.7$ in the wCDM model to evaluate δ_d and $\Delta_d = \frac{\delta_d}{\delta_m}$, the

[1] Since we are in the linear regime we verify that for different values of k the differences in $f\sigma_8$ are practically negligible ($\sim 10^{-5}$ per cent).

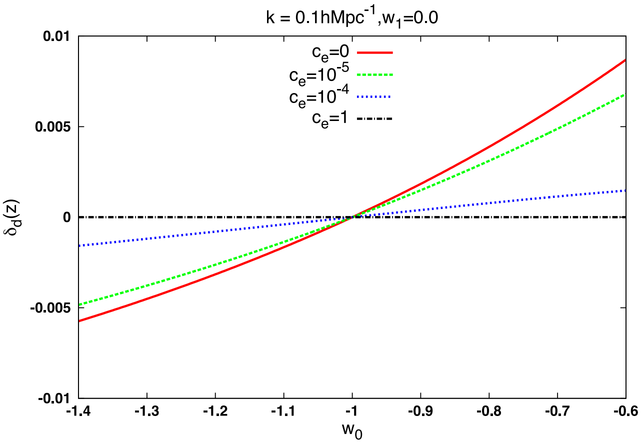

Figure 1. The density contrast of DE as a function of the EoS at the present time for four different values of the sound speed. The red solid curve shows a fully clustering DE model with $c_e = 0$. The green dashed (blue dotted) curve is for $c_e = 10^{-5}$ ($c_e = 10^{-4}$). A non-clustering model with $c_e = 1$ is shown by a black dashed–dotted line.

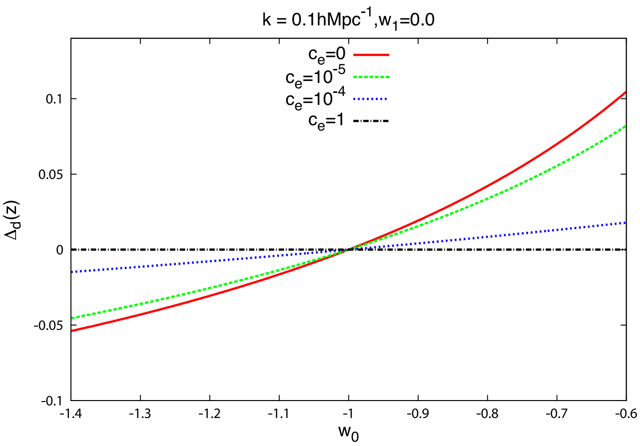

Figure 2. The relative density contrast of DE as a function of the EoS at the present time for four different values of the sound speed. Line style and colours are as in Fig. 1.

relative DE density contrast, for a few distinct values of the DE sound speed as a function of the EoS. In Fig. 1 the density contrast of DE as a function of w_d at the present time is presented. The non-clustering case remains homogeneous but for small values of the DE sound speed, the density contrast grows while increasing the EoS. In contrast to the non-clustering case, the fully clustering regime with $c_e = 0$ gives a maximum value for the DE density contrast. In Fig. 2 the relative DE density contrast is shown as a function of EoS. The behaviour of this quantity is similar to that of the density contrast.

As we stated the quantity $f\sigma_8(z)$ is affected by DE clustering. To show how $f\sigma_8(z)$ changes with the DE sound speed, we evaluate $\Delta f\sigma_8(z) = \frac{f_h\sigma_{8,h}(z) - f\sigma_8(z)}{f\sigma_8(z)} \times 100$ and $\Delta\gamma(z) = \frac{\gamma_h(z) - \gamma(z)}{\gamma(z)} \times 100$ as a function of the EoS parameter. In the previous equations, h stands for homogeneous DE. For the growth rate, results at present time are presented in Fig. 3. As expected, the deviation increases by increasing the EoS and for $w_d < -0.9$ the difference is less than 1 per cent. The relative difference between homogeneous and clustering DE for the growth index $\Delta\gamma(z = 0)$ has been shown in Fig. 4. The difference between the homogeneous and the clustering DE models is also very small for w_d very close to the ΛCDM model.

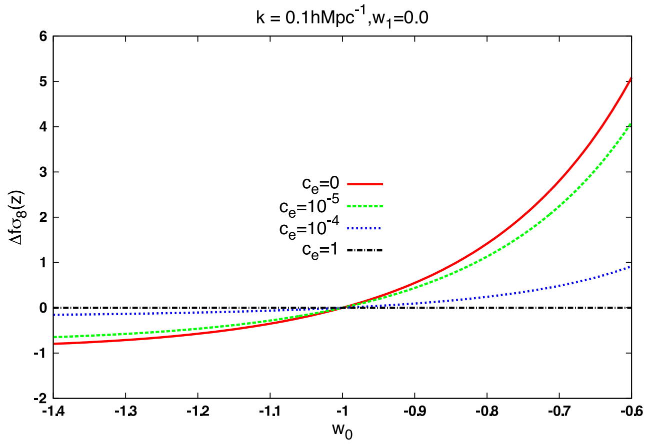

Figure 3. The relative difference of $f\sigma_8$ at the present time as a function of EoS. Line style and colours are as in Fig. 1.

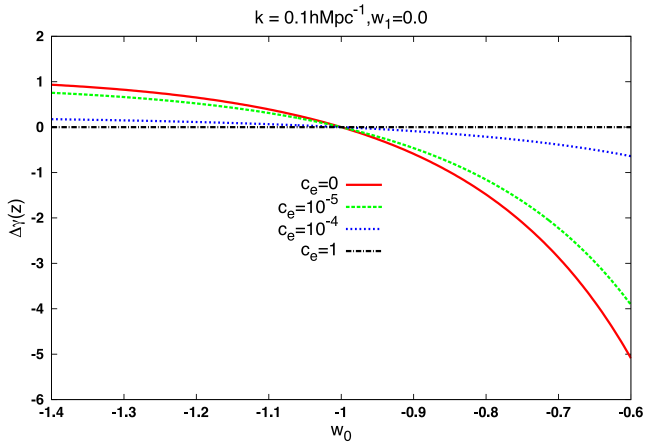

Figure 4. The relative difference of the growth index at present time as a function of EoS. Line style and colours are as in Fig. 1.

3 OBSERVATIONAL CONSTRAINTS ON THE DE SOUND SPEED

In this section we use current available observational data sets to constrain the cosmological background parameters and the DE sound speed. In this analysis we assume that the DE sound speed is constant in time, regardless of the particular EoS parameter adopted. Our cosmological model will be described by the following parameters: Ω_m^0 (matter density), Ω_b^0 (baryon density), $h = H_0/100$ (normalized Hubble constant), w_0 and w_1 (DE EoS parameters) and c_e (effective sound speed) to describe the DE perturbations. In our analysis we assume a flat universe so that $\Omega_{DM} + \Omega_b + \Omega_d = 1$, hence the amount of DE is known from the knowledge of the matter and baryon density parameters.

The first data set we consider is the SnIa distance module from Union 2.1 sample (Suzuki et al. 2012). This data set includes 580 SnIa and its χ^2 is given by

$$\chi^2_{sn} = \sum_i \frac{[\mu_{th}(z_i) - \mu_{ob}(z_i)]^2}{\sigma_i^2}, \tag{18}$$

where $\mu_{th}(z) = 5\log_{10}\left[(1+z)\int_0^z \frac{dx}{E(x)}\right] + \mu_0$, $\mu_0 = 42.384 - 5\log_{10}h$ and σ_i are the corresponding uncertainties. Before finding the minimum of χ^2_{sn} we can expand χ^2_{sn} around μ_0

$$\chi^2_{sn} = A + 2B\mu_0 + C\mu_0^2, \tag{19}$$

Table 1. The current available BAO data which we use in our analysis.

z	d_i	Survey and references
0.106	0.336	6dF (Beutler et al. 2011)
0.35	0.113	SDSS-DR7 (Padmanabhan et al. 2012)
0.57	0.073	SDSS-DR9 (Anderson et al. 2013)
0.44	0.0916	WiggleZ (Blake et al. 2011)
0.6	0.0726	WiggleZ (Blake et al. 2011)
0.73	0.0592	WiggleZ (Blake et al. 2011)

where

$$A = \sum_i \frac{[\mu_{\rm th}(\mu_0 = 0) - \mu_{\rm ob}]^2}{\sigma_i^2},$$
$$B = \sum_i \frac{[\mu_{\rm th}(\mu_0 = 0) - \mu_{\rm ob}]}{\sigma_i^2},$$
$$C = \sum_i \frac{1}{\sigma_i^2}.$$

Obviously, for $\mu_0 = -B/C$ equation (19) has a minimum, namely $A - \frac{B^2}{C}$. Now by defining $\tilde{\chi}^2_{\rm sn} = A - \frac{B^2}{C}$, we can use the minimum of $\tilde{\chi}^2_{\rm sn}$ which is independent of μ_0 in order to find the best values of the parameters. Of course both estimators provide the same results (Nesseris & Perivolaropoulos 2005).

The second data set we consider is the BAO sample which includes six distinct measurements of the baryon acoustic scale. These six data points and their references are summarized in Table 1. To find the $\chi^2_{\rm BAO}$ we follow the same procedure as Hinshaw et al. (2013). So the $\chi^2_{\rm BAO}$ is given by

$$\chi^2_{\rm BAO} = \mathbf{Y}^{\rm T}\mathbf{C}^{-1}_{\rm BAO}\mathbf{Y}, \tag{20}$$

where $\mathbf{Y} = (d(0.1) - d_1, \frac{1}{d(0.35)} - \frac{1}{d_2}, \frac{1}{d(0.57)} - \frac{1}{d_3}, d(0.44) - d_4, d(0.6) - d_5, d(0.73) - d_6)$ and

$$d(z) = \frac{r_{\rm s}(z_{\rm drag})}{D_V(z)}, \tag{21}$$

with

$$r_{\rm s}(a) = \int_0^a \frac{c_{\rm s}(a){\rm d}a}{a^2 H(a)}, \tag{22}$$

is the comoving sound horizon at the baryon drag epoch, $c_{\rm s}(a)$ the baryon sound speed and $D_V(z)$ is defined by

$$D_V(z) = \left[(1+z)^2 D_{\rm A}^2(z)\frac{z}{H(z)}\right]^{1/3}, \tag{23}$$

and $D_{\rm A}(z)$ is the angular diameter distance. We used the fitting formula for $z_{\rm d}$ from Eisenstein & Hu (1998) and the baryon sound speed is given by

$$c_{\rm s}(a) = \frac{1}{\sqrt{3(1 + \frac{3\Omega_b^0}{4\Omega_\gamma^0}a)}}, \tag{24}$$

where we set $\Omega_\gamma^0 = 2.469 \times 10^{-5} h^{-2}$ (Hinshaw et al. 2013). The covariance matrix $\mathbf{C}^{-1}_{\rm BAO}$ in equation (20) was obtained by Hinshaw et al. (2013)

$$\begin{pmatrix} 4444.4 & 0.0 & 0.0 & 0.0 & 0.0 & 0.0 \\ 0.0 & 34.602 & 0.0 & 0.0 & 0.0 & 0.0 \\ 0.0 & 0.0 & 20.6611 & 0.0 & 0.0 & 0.0 \\ 0.0 & 0.0 & 0.0 & 24\,532.1 & -25\,137.7 & 12\,099.1 \\ 0.0 & 0.0 & 0.0 & -25\,137.7 & 134\,598.4 & -64\,783.9 \\ 0.0 & 0.0 & 0.0 & 12\,099.1 & -64\,783.9 & 128\,837.6 \end{pmatrix}.$$

The position of the CMB acoustic peak provides useful data to constrain DE models. The position of this peak is given by ($l_{\rm a}$, R, z_*), where R is the scale distance to recombination

$$l_a = \pi \frac{D_{\rm A}(z_*)}{r_s(z_*)}, \tag{25}$$

$$R = \sqrt{\Omega_{\rm m}^0} H_0 D_{\rm A}(z_*), \tag{26}$$

and $r_{\rm s}(z)$ is the comoving sound horizon defined in equation (22). In this case we used the formula for z_* from Hu & Sugiyama (1996). For the *WMAP* data set we have (Hinshaw et al. 2013)

$$\mathbf{X}_{\rm CMB} = \begin{pmatrix} l_{\rm a} - 302.40 \\ R - 1.7264 \\ z_* - 1090.88 \end{pmatrix}, \tag{27}$$

and

$$\mathbf{C}^{-1}_{\rm CMB} = \begin{pmatrix} 3.182 & 18.253 & -1.429 \\ 18.253 & 11\,887.879 & -193.808 \\ -1.429 & -193.808 & 4.556 \end{pmatrix}. \tag{28}$$

In addition to this data set the *Planck* data provide more accurate CMB data for which the position of the acoustic peak is given by (Shafer & Huterer 2014)

$$\mathbf{X}_{\rm CMB} = \begin{pmatrix} l_{\rm a} - 301.65 \\ R - 1.7499 \\ z_* - 1090.41 \end{pmatrix}, \tag{29}$$

and

$$\mathbf{C}^{-1}_{\rm CMB} = \begin{pmatrix} 42.7044 & -418.36 & -0.7820 \\ -418.36 & 573\,66.3 & -762.152 \\ -0.7820 & -762.152 & 14.6995 \end{pmatrix}. \tag{30}$$

In both cases the $\chi^2_{\rm CMB}$ is given by

$$\chi^2_{\rm CMB} = \mathbf{X}^{\rm T}_{\rm CMB}\mathbf{C}^{-1}_{\rm CMB}\mathbf{X}_{\rm CMB}. \tag{31}$$

A further data set used in this work is the Hubble evolution data obtained from the evolution of galaxies (Simon, Verde & Jimenez 2005). We use the 12 available data points and the χ^2 for this data set is

$$\chi^2_{\rm H} = \sum_i \frac{[H(z_i) - H_{\rm ob,i}]^2}{\sigma_i^2}. \tag{32}$$

The BBN provides a data point (Burles, Nollett & Turner 2001; Serra et al. 2009) which constrains mostly $\Omega_{\rm b}^0$. The $\chi^2_{\rm BBN}$ is given by

$$\chi^2_{\rm BBN} = \frac{(\Omega_{\rm b}^0 h^2 - 0.022)^2}{0.002^2}. \tag{33}$$

The final data set used is the growth rate data. These data were derived from RSDs from galaxy surveys including PSCs, 2DF, VVDS, SDSS, 6dF, 2MASS, BOSS and WiggleZ and the data with their references are shown in Table 2. We solve equations (10) and (11) numerically to find $f(z)\sigma_8(z)$ and compute $\chi^2_{\rm fs}$ with

$$\chi^2_{\rm fs} = \sum_i \frac{[f\sigma_8(z_i) - f\sigma_{8,\rm ob}]^2}{\sigma_i^2}. \tag{34}$$

The overall likelihood function is given by the product of the individual likelihoods:

$$\mathcal{L}_{\rm tot} = \mathcal{L}_{\rm sn} \times \mathcal{L}_{\rm BAO} \times \mathcal{L}_{\rm CMB} \times \mathcal{L}_{\rm H} \times \mathcal{L}_{\rm BBN} \times \mathcal{L}_{\rm fs}, \tag{35}$$

and the total chi-square $\chi^2_{\rm tot}$ is given by

$$\chi^2_{\rm tot} = \chi^2_{\rm sn} + \chi^2_{\rm BAO} + \chi^2_{\rm CMB} + \chi^2_{\rm H} + \chi^2_{\rm BBN} + \chi^2_{\rm fs}. \tag{36}$$

Table 2. The $f\sigma_8(z)$ data points including their references and surveys.

z	$f\sigma_8(z)$	Reference
0.02	0.360 ± 0.040	Hudson & Turnbull (2013)
0.067	0.423 ± 0.055	Beutler et al. (2012)
0.10	0.37 ± 0.13	Feix, Nusser & Branchini (2015)
0.17	0.510 ± 0.060	Percival et al. (2004)
0.35	0.440 ± 0.050	Song & Percival (2009); Tegmark et al. (2006)
0.77	0.490 ± 0.180	Guzzo et al. (2008); Song & Percival (2009)
0.25	0.351 ± 0.058	Samushia, Percival & Raccanelli (2012)
0.37	0.460 ± 0.038	Samushia et al. (2012)
0.22	0.420 ± 0.070	Blake et al. (2011)
0.41	0.450 ± 0.040	Blake et al. (2011)
0.60	0.430 ± 0.040	Blake et al. (2011)
0.60	0.433 ± 0.067	Tojeiro et al. (2012)
0.78	0.380 ± 0.040	Blake et al. (2011)
0.57	0.427 ± 0.066	Reid et al. (2012)
0.30	0.407 ± 0.055	Tojeiro et al. (2012)
0.40	0.419 ± 0.041	Tojeiro et al. (2012)
0.50	0.427 ± 0.043	Tojeiro et al. (2012)
0.80	0.47 ± 0.08	de la Torre et al. (2013)

Table 3. The best value parameters and their 1σ uncertainty for the wCDM model.

Parameters	Best (*WMAP*)	Best (*Planck*)
h	$0.6955^{+0.0040}_{-0.0037}$	$0.7064^{+0.0011}_{-0.0012}$
$\Omega^0_{\rm DM}$	$0.2273^{+0.0027}_{-0.0029}$	$0.2361^{+0.0010}_{-0.0010}$
$\Omega^0_{\rm b}$	$0.0470^{+0.0004}_{-0.0005}$	$0.0482^{+0.0003}_{-0.0002}$
w_0	$-0.9436^{+0.0144}_{-0.0141}$	$-0.9975^{+0.0055}_{-0.0053}$
$c_{\rm e}$	0.0	0.001
σ_8	0.837	0.829

Table 4. The best value parameters and their 1σ uncertainty for the w(t)CDM model.

Parameters	Best (*WMAP*)	Best (*Planck*)
h	$0.7001^{+0.0040}_{-0.0038}$	$0.7070^{+0.0012}_{-0.0013}$
$\Omega^0_{\rm DM}$	$0.2234^{+0.0028}_{-0.0027}$	$0.2361^{+0.0012}_{-0.0011}$
$\Omega^0_{\rm b}$	$0.0474^{+0.0005}_{-0.0005}$	$0.0481^{+0.0003}_{-0.0003}$
w_0	$-1.0176^{+0.0128}_{-0.0124}$	$-0.95204^{+0.0060}_{-0.0058}$
w_1	$0.3289^{+0.0395}_{-0.0405}$	$-0.18512^{+0.0205}_{-0.0195}$
$c_{\rm e}$	0.002	0.0
σ_8	0.840	0.829

Table 5. The best value parameters and their 1σ uncertainty for the ΛCDM model.

Parameters	Best (*WMAP*)	Best (*Planck*)
h	$0.7048^{+0.0042}_{-0.0041}$	$0.7069^{+0.0011}_{-0.0010}$
$\Omega^0_{\rm DM}$	$0.2261^{+0.0030}_{-0.0029}$	$0.2359^{+0.0010}_{-0.0011}$
$\Omega^0_{\rm b}$	$0.0456^{+0.0006}_{-0.0005}$	$0.0481^{+0.0003}_{-0.0003}$
σ_8	0.839	0.829

We calculate the total chi-square $\chi^2_{\rm tot}$ and find the best value of the parameters with an MCMC algorithm. The number of degrees of freedom is $\nu = N - n_{\rm fit} - 1$, where $N = 616$ and $n_{\rm fit}$ is the number of the fitted parameters. The results of this analysis for the wCDM, w(t)CDM and ΛCDM are summarized in Tables 3, 4 and 5, respectively.

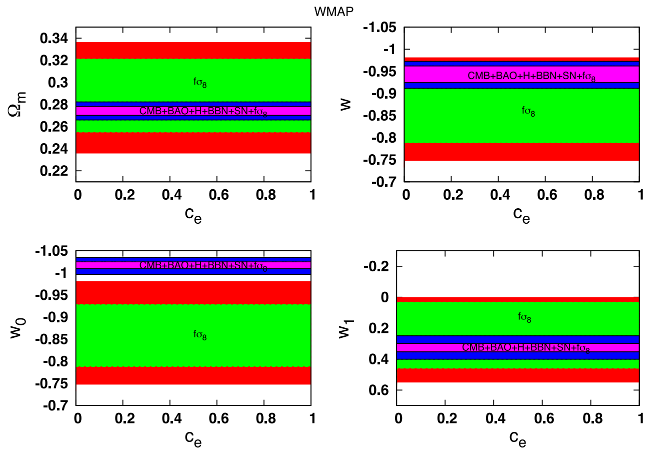

Figure 5. The 1σ and 2σ contours of $\Omega_{\rm m}$(wCDM), w(wCDM), w_0(w(t)CDM) and w_1(w(t)CDM) versus DE sound speed using *WMAP* data. The 1σ and 2σ contours correspond to $\chi^2 - \chi^2_{\rm b} = 2.3$ and $\chi^2 - \chi^2_{\rm b} = 6.16$. The green (red) area correspond to 1σ (2σ) using only $f\sigma_8$ data and purple (blue) show 1σ (2σ) using all data set.

To compare the DE models we have computed the corrected Akaike information criterion (AIC) (Akaike 1974; Sugiura 1978) which, in our case, due to $N/n_{\rm fit} > 40$, is given by

$$\mathrm{AIC} = \chi^2_{\rm min} + 2n_{\rm fit}. \tag{37}$$

A smaller value of AIC indicates a better model-data fit. Of course, it is well known that small differences in AIC are not necessarily significant and therefore, in order to assess the effectiveness of the different models in reproducing the data, we need to estimate the model pair difference $\Delta\mathrm{AIC} = \mathrm{AIC}_y - \mathrm{AIC}_x$. The higher the value of $|\Delta\mathrm{AIC}|$, the higher the evidence against the model with a higher value of AIC. With a difference $|\Delta\mathrm{AIC}| \geq 2$ indicating a positive evidence and $|\Delta\mathrm{AIC}| \geq 6$ indicating a strong evidence, while a value $|\Delta\mathrm{AIC}| \leq 2$ indicates consistency among the two models. The results of our analysis are the following.

(i) Using *WMAP* data:

(a) For the wCDM model, $\chi^2_{\rm min} = 586.53$, $n_{\rm fit} = 5$, so AIC = 596.53

(b) For the w(t)CDM model, $\chi^2_{\rm min} = 585.32$, $n_{\rm fit} = 6$, so AIC = 597.32

(c) For the ΛCDM model, $\chi^2_{\rm min} = 589.22$, $n_{\rm fit} = 3$, so AIC = 595.32.

(ii) Using Planck data:

(a) For the wCDM model, $\chi^2_{\rm min} = 595.76$, $n_{\rm fit} = 5$, so AIC = 605.76

(b) For the w(t)CDM model, $\chi^2_{\rm min} = 595.50$, $n_{\rm fit} = 6$, so AIC = 607.50

(c) For the ΛCDM model, $\chi^2_{\rm min} = 595.79$, $n_{\rm fit} = 3$, so AIC = 601.79.

Concerning the best value of the DE sound speed we find that it tends to zero but the corresponding error bars remain quite large within 1σ. In particular $c_{\rm e}$ lies in the range $\in [0, 1]$.

In order to investigate the range of validity for $c_{\rm e}$, in Figs 5 and 6 we provide the 1σ and 2σ contours of our analysis. Note that in both plots the upper panels are for wCDM in which we present the confidence levels in the $(c_{\rm e}, \Omega_{\rm m})$ and $(c_{\rm e}, w)$ planes, where $\Omega_{\rm m} = \Omega^0_{\rm DM} + \Omega^0_{\rm b}$. In the bottom panels of Figs 5 and 6 the contours for w_0 and w_1 in the CPL model are shown with respect to the

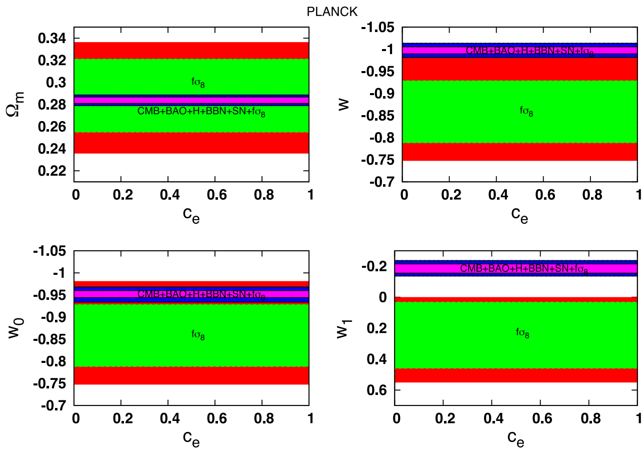

Figure 6. Same as Fig. 5 but using the *Planck* shift parameter.

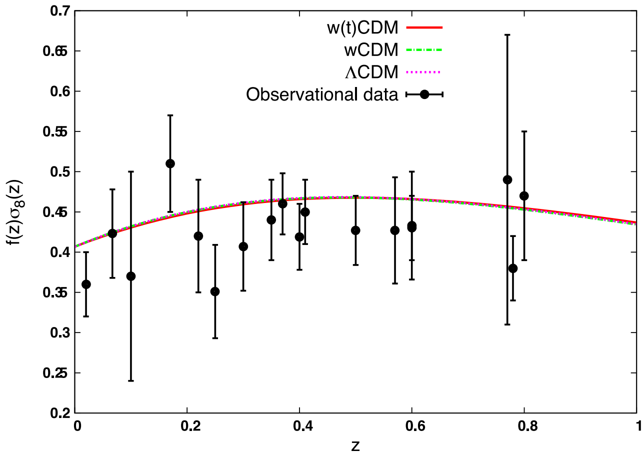

Figure 7. The $f\sigma_8(z)$ quantity (using *Planck* data), for the best values cosmological parameters for the wCDM (green dot–dashed curve) and w(t)CDM (red solid curve) models. The ΛCDM model is shown by the violet short dashed curve.

DE sound speed. From this analysis it becomes clear that there is a strong degeneracy between c_e and (Ω_m, w) which implies that all values in the interval $0 \leq c_e \leq 1$ are acceptable within the 1σ uncertainty.

In Figs 7 and 8 we present the quantity $f\sigma_8(z)$ for our best value parameters by considering the *Planck* and *WMAP* data for the wCDM, w(t)CDM and the ΛCDM models, respectively. We also show the observational data points. In addition to this quantity in Figs 9 and 10 the growth index for the best values of the parameters have been shown. Note that using *Planck* CMB data our likelihood analysis indicates that all three models are very close to each other.[2]

Previous works in literature tried to put constraints on the DE effective sound speed c_e using different kind of data. de Putter et al. (2010) used a combination of CMB temperature power spectrum data, their cross-correlation with several mass-density tracers and the SDSS LRG auto-correlation function. Supernovae data were used to break degeneracies with background cosmological parameters. Hannestad (2005) used a set of supernova data, LSS and CMB power spectra. Finally, Xia et al. (2008) performed a similar analysis for a single perfect fluid and a two-field Quintom DE model with

[2] See the results of χ^2 for the *Planck* case.

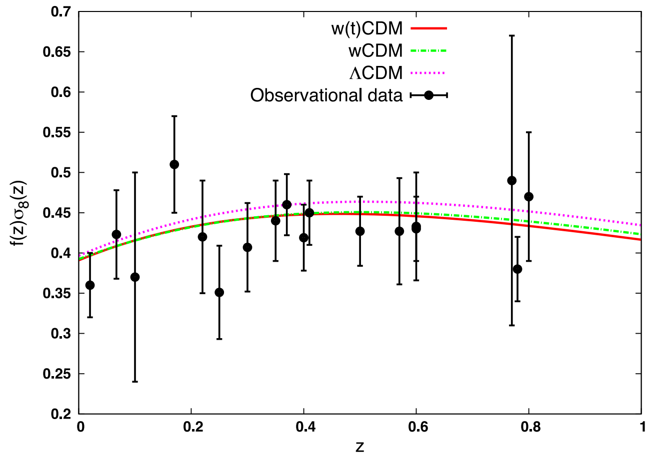

Figure 8. The $f\sigma_8(z)$ quantity (using *WMAP* data), for the best values cosmological parameters for the wCDM (green dot–dashed curve) and w(t)CDM (red solid curve) models. The ΛCDM model is shown by the violet short dashed curve.

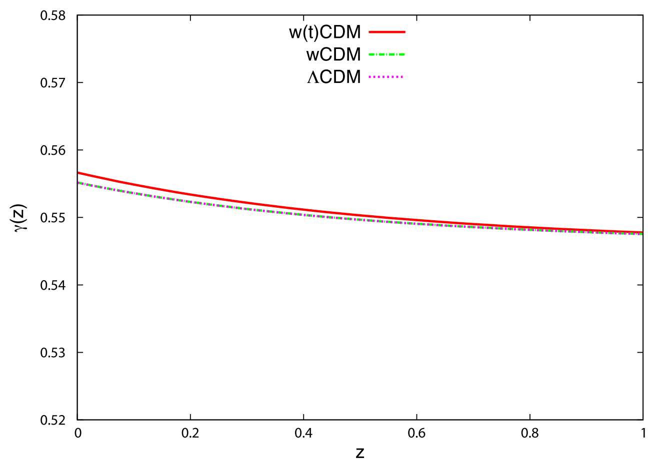

Figure 9. The growth index (using *Planck* data), for the best values cosmological parameters for the wCDM (green dot–dashed curve) and w(t)CDM (red solid curve) models. The ΛCDM model is shown by the violet short dashed curve.

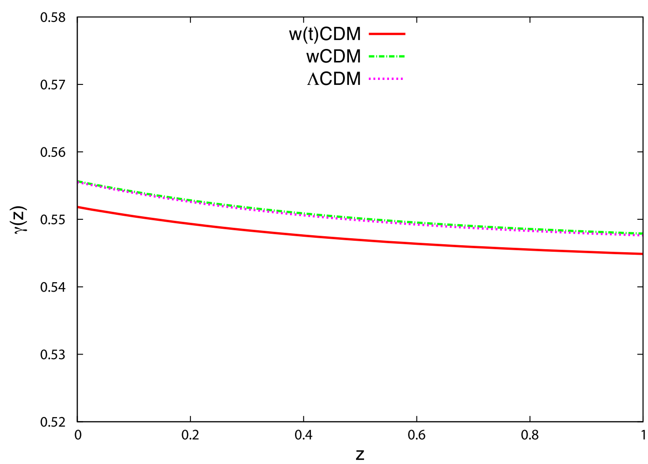

Figure 10. The growth index (using *WMAP* data), for the best values cosmological parameters for the wCDM (green dot–dashed curve) and w(t)CDM (red solid curve) models. The ΛCDM model is shown by the violet short dashed curve.

$w = -1$ crossing by analysing CMB anisotropy data, LSS and SNIa observational data. In all these studies, using a similar approach to the one used in this work, the authors reach our same results. While previous and current data can constrain at a good level the current EoS parameter of the DE component, the quality of the observations is unfortunately still not sufficient enough to put any constraint on the DE effective sound speed. Note, however, that this is also due to the negligible contribution of DE at early times on one side, and to the fact that current observations favour $w \simeq -1$. As pointed out by de Putter et al. (2010), if one considers the case of early DE models (Doran & Robbers 2006) where the contribution of DE at early times, i.e. CMB, is not negligible, then more stringent limits can be set on c_e.

4 GROWTH INDEX ANALYTIC SOLUTION

In Section 2 we investigated the evolution of the growth index by solving numerically the system of equations (5), (10) and (11). Here our aim is to extend the work of Basilakos (2015) in order to provide a general $\gamma(z)$ approximated solution which can be used in studies of structure formation. On sub-horizon scales, namely $\frac{k^2}{a^2} \gg H^2$ (or $k^2 \gg \mathcal{H}^2$), Poisson equation (see Appendix B) takes the form

$$-\frac{k^2}{a^2}\phi = \frac{3H^2}{2}\left[\Omega_m\delta_m + \Omega_d\delta_d(1+3c_e)\right]. \tag{38}$$

Under the above conditions, equation (10) becomes

$$a^2\frac{d^2\delta_m}{da^2} + a\left(3+\frac{\dot{H}}{H^2}\right)\frac{d\delta_m}{da} = \frac{3}{2}\left[\Omega_m\delta_m + (1+3c_e)\Omega_d\delta_d\right] \tag{39}$$

In this framework, for $\delta_d = 0$, the latter equation reduces to the well-known scale-independent equation which is also valid for the concordance Λ cosmology.

Concerning the EoS parameter, it is well known that one can express it in terms of the Hubble parameter (Saini et al. 2000; Huterer & Turner 2001)

$$w_d(a) = \frac{-1-\frac{2}{3}a\frac{d\ln H}{da}}{1-\Omega_m(a)}, \tag{40}$$

or

$$a\frac{d\ln H}{da} = \frac{\dot{H}}{H^2} = -\frac{3}{2} - \frac{3}{2}w_d(a)\Omega_d(a), \tag{41}$$

where $\Omega_m(a) = 1 - \Omega_d(a) = \frac{\Omega_{m0}}{a^3E^2(a)}$ and $E(a) = H(a)/H_0$. Now, substituting equation (41) and $f = \mathrm{d}\ln\delta_m/\mathrm{d}\ln a$ into equation (39) we obtain the basic differential equation which governs the growth rate of clustering

$$a\frac{df}{da} + f^2 + \left(\frac{1}{2} - \frac{3}{2}w_d\Omega_d\right)f = \frac{3}{2}\left[\Omega_m + (1+3c_e)\Delta_d\Omega_d\right] \tag{42}$$

where $\Delta_d(a) \equiv \delta_d/\delta_m$. To this end, changing the variables in equation (42) from $a(z)$ to redshift $[\frac{df}{da} = -(1+z)^{-2}\frac{df}{dz}]$ and utilizing $f(z) = \Omega_m(z)^{\gamma(z)}$ we arrive to

$$-(1+z)\gamma_z\ln(\Omega_m) + \Omega_m^{\gamma} + 3w_d\Omega_d\left(\gamma - \frac{1}{2}\right) + \frac{1}{2} = \frac{3}{2}\Omega_m^{1-\gamma}X \tag{43}$$

where $\gamma_z = \mathrm{d}\gamma/\mathrm{d}z$ and

$$X(z) = 1 + \frac{\Omega_d(z)}{\Omega_m(z)}\Delta_d(z)(1+3c_e). \tag{44}$$

On the other hand, the parametrization $f(a) = \mathrm{d}\ln\delta_m/\mathrm{d}\ln a \simeq \Omega_m(a)^{\gamma(a)}$ has a great impact in cosmological studies because it can be used in order to simplify the numerical calculations of equation (39). Obviously, a direct integration gives

$$\delta_m(a,\gamma) = a(z)\exp\left[\int_{a_i}^{a(z)}\frac{du}{u}\left(\Omega_m^{\gamma}(u)-1\right)\right], \tag{45}$$

where $a(z) = 1/(1+z)$ and a_i is the scale factor of the universe at which the matter component dominates the cosmic fluid (here we use $a_i \simeq 10^{-1}$ or $z_i \simeq 10$). Hence, the linear growth factor normalized to unity at the present epoch is $D(a) = \frac{\delta_m(a,\gamma)}{\delta_m(1,\gamma)}$. Therefore, in order to proceed with the analysis we need to somehow know the functional form of $\gamma(z)$. From the phenomenological point of view we may parametrize $\gamma(z)$ as follows:

$$\gamma(z) = \gamma_0 + \gamma_1 y(z). \tag{46}$$

This equation can be seen as a first-order Taylor expansion around some cosmological quantity such as $a(z)$ and z.

Recently, it has been found (Basilakos 2012; Basilakos & Pouri 2012, and references therein) that for those $y(z)$ functions which satisfy the condition $y(0) = 0$ [or $\gamma(0) = \gamma_0$], the parameter γ_1 is written as a function of γ_0. For example, at the present epoch $[z = 0, \gamma_z(0) = \gamma_1 y_z(0), X_0 = X(0), w_0 = w_d(0)]$, equation (43) is written as

$$\gamma_1 = \frac{\Omega_{m0}^{\gamma_0} + 3w_0(\gamma_0 - \frac{1}{2})\Omega_{d0} + \frac{1}{2} - \frac{3}{2}\Omega_{m0}^{1-\gamma_0}X_0}{y_z(0)\ln\Omega_{m0}}, \tag{47}$$

where $y_z = \mathrm{d}y/\mathrm{d}z$. Note that a similar equation has been found in Basilakos (2015) in the case of $c_e \equiv w_d$ with $w_d = $ const. As it is expected, for the homogeneous DE case ($\Delta_d = 0, X = 1$), we verify that the above formula boils down to that of Polarski & Gannouji (2008) for $y(z) = z$. Within this framework, assuming $y(z) = 1 - a(z) = \frac{z}{1+z}$ (Ballesteros & Riotto 2008), we fully recover results in literature (Ishak & Dossett 2009; Bueno Belloso, García-Bellido & Sapone 2011; di Porto, Amendola & Branchini 2012). Notice that below we focus on $y(z) = 1 - a(z) = \frac{z}{1+z}$ with $y_z(0) = 1$. The fact that $\Omega_d(z) \simeq 0$ at $z \gg 1$ implies that the asymptotic value of the growth index $\gamma_\infty = \gamma_0 + \gamma_1$ is not really affected by the DE clustering. Therefore, plugging $\gamma_0 = \gamma_\infty - \gamma_1$[3] into equation (47) we can obtain the constants $\gamma_{0,1}$ in terms of (Ω_{m0}, w_0, Δ_{d0}, c_e). In Fig. 11 we present (γ_0, γ_1) as a function of Δ_{d0}. The curves are constructed using the parameters from Tables 3 and 4 (third column) and they correspond to w(t)CDM (solid) and wCDM (dashed) models. We observe that for $\Delta_{d0} > 0$ the growth index starts to deviate from that of the ΛCDM model, namely $\gamma_0 < 0.55$ and $\gamma_1 > 0$. In the case of $\Delta_{d0} < 0$ the value of γ_0 is greater than that of the homogeneous case ($\gamma_0 > 0.55$). In this context, concerning the value of γ_1 we find that it becomes negative. Of course for $\Delta_{d0} = 0$ the pair (γ_0, γ_1) reduces to that of the homogeneous case (see solid points in Fig. 11), as it should.

5 CONCLUSIONS

To summarize, we study the impact of DE clustering on the growth index of matter fluctuations. Initially we provide the most general form of the equations governing DM and DE clustering within the framework of $c_e = $ const. Then using the well-known EoS parameters, namely $w_d(z) = w_0 + w_1 z/(1+z)$, $w_d(z) = $ const and the

[3] Regarding the asymptotic value of the growth index we use $\gamma_\infty \approx 3(w - 1)/(6w - 5)$ for the wCDM model (see Linder & Cahn 2007; Nesseris & Perivolaropoulos 2008) and $\gamma_\infty \approx 0.55 + 0.05[1 + w(z = 1)]$ for the w(t)CDM model (Linder 2005).

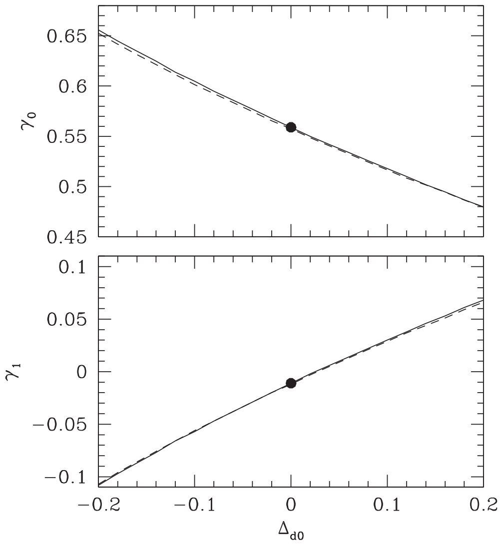

Figure 11. The pair (γ_0, γ_1) as a function of Δ_{d0}. The solid and the dashed lines correspond to the w(t)CDM and wCDM DE models, respectively. The homogeneous case $\Delta_{d0} = 0$ is shown by the solid point. For the cosmological parameters, we use the values of Tables 3 and 4 (third column).

current cosmological data we place constrains on the cosmological parameters, including that of the effective sound speed c_e. Although the likelihood function peaks at $c_e \sim 0$, which indicates that the DE component clusters in analogy to the matter component $c_e \sim 0$, the corresponding error bars are quite large within 1σ uncertainties which implies that c_e remains practically unconstrained. We also compared our findings with previous work reaching the same conclusion that at the moment the quality of cosmological data is not sufficient enough to put constraint on the DE effective sound speed. Future cosmological data, based for example on *Euclid*, are expected to improve even further the relevant constraints on c_e and thus the validity of clustered DE will be effectively tested. Finally, we have derived a new approximated solution of the growth index in terms of the cosmological parameters, DE perturbations and c_e.

ACKNOWLEDGEMENTS

We thank the anonymous referee whose comments helped to improve the paper.

REFERENCES

Abramo L., Batista R., Liberato L., Rosenfeld R., 2009, Phys. Rev. D, 79, 023516
Akaike H., 1974, IEEE Trans. Autom. Control, 19, 716
Akhoury R., Garfinkle D., Saotome R., 2011, J. High Energy Phys., 1104, 096
Amendola L., Tsujikawa S., 2010, Dark Energy: Theory and Observations. Cambridge Univ. Press, Cambridge
Anderson L. et al., 2013, MNRAS, 427, 3435
Armendariz-Picon C., Damour T., Mukhanov V. F., 1999, Phys. Lett. B, 458, 209
Armendariz-Picon C., Mukhanov V. F., Steinhardt P. J., 2000, Phys. Rev. Lett., 85, 4438
Astier P. et al., 2006, A&A, 447, 31
Babichev E., Mukhanov V. F., Vikman A., 2006, J. High Energy Phys., 0609, 061
Ballesteros G., Riotto A., 2008, Phys. Lett. B, 668, 171
Basilakos S., 2012, Int. J. Mod. Phys. D, 21, 50064
Basilakos S., 2015, MNRAS, 449, 2151
Basilakos S., Pouri A., 2012, MNRAS, 423, 3761
Basilakos S., Bueno Sanchez J., Perivolaropoulos L., 2009, Phys. Rev. D, 80, 043530
Basse T., Bjaelde O. E., Hamann J., Hannestad S., Wong Y. Y., 2014, J. Cosmol. Astropart. Phys., 1405, 021
Batista R. C., 2014, Phys. Rev. D, 89, 123508
Batista R., Pace F., 2013, J. Cosmol. Astropart. Phys., 1306, 044
Bean R., Doré O., 2004, Phys. Rev. D, 69, 083503
Bennett C. et al., 2003, ApJS, 148, 1
Beutler F. et al., 2011, MNRAS, 416, 3017
Beutler F. et al., 2012, MNRAS, 423, 3430
Blake C. et al., 2011a, MNRAS, 415, 2876
Blake C. et al., 2011b, MNRAS, 418, 1707
Bueno Belloso A., García-Bellido J., Sapone D., 2011, J. Cosmol. Astropart. Phys., 10, 10
Burles S., Nollett K. M., Turner M. S., 2001, ApJ, 552, L1
Capozziello S., Carloni S., Troisi A., 2003, in Pandalai S. G., ed., Recent Research Developments in Astronomy and Astrophysics, Vol. 1, Research Signpost, Trivandrum, p. 625
Carroll S. M., Duvvuri V., Trodden M., Turner M. S., 2004, Phys. Rev. D, 70, 043528
Chevallier M., Polarski D., 2001, Int. J. Mod. Phys. D, 10, 213
Chiba T., Okabe T., Yamaguchi M., 2000, Phys. Rev. D, 62, 023511
Chiba T., Dutta S., Scherrer R. J., 2009, Phys. Rev. D, 80, 043517
Cole S. et al., 2005, MNRAS, 362, 505
Copeland E. J., Sami M., Tsujikawa S., 2006, Int. J. Mod. Phys. D, 15, 1753
de la Torre S. et al., 2013, A&A, 557, A54
de Putter R., Huterer D., Linder E. V., 2010, Phys. Rev. D, 81, 103513
di Porto C., Amendola L., Branchini E., 2012, MNRAS, 419, 985
Dobado A., Maroto A. L., 1995, Phys. Rev. D, 52, 1895
Doran M., Robbers G., 2006, J. Cosmol. Astropart. Phys., 6, 26
Dossett J., Ishak M., 2013, Phys. Rev. D, 88, 103008
Dvali G., Gabadadze G., Porrati M., 2000, Phys. Lett. B, 485, 208
Eisenstein D. J., Hu W., 1998, ApJ, 496, 605
Eisenstein D. J. et al., 2005, ApJ, 633, 560
Erickson J. K., Caldwell R., Steinhardt P. J., Armendariz-Picon C., Mukhanov V. F., 2002, Phys. Rev. Lett., 88, 121301
Feix M., Nusser A., Branchini E., 2015, Phys. Rev. Lett., 115, 1301
Garriga J., Mukhanov V. F., 1999, Phys. Lett. B, 458, 219
Guzzo L. et al., 2008, Nature, 451, 541
Hannestad S., 2005, Phys. Rev. D, 71, 103519
Hawkins E. et al., 2003, MNRAS, 346, 78
Hinshaw G. et al., 2013, ApJS, 208, 19
Hu W., 1998, ApJ, 506, 485
Hu W., Scranton R., 2004, Phys. Rev. D, 70, 123002
Hu W., Sugiyama N., 1996, ApJ, 471, 542
Hudson M. J., Turnbull S. J., 2013, ApJ, 751, L30
Huterer D., Linder E. V., 2007, Phys. Rev. D, 75, 023519
Huterer D., Turner M. S., 2001, Phys. Rev. D, 64, 123527
Ishak M., Dossett J., 2009, Phys. Rev. D, 80, 043004
Jha S., Riess A. G., Kirshner R. P., 2007, ApJ, 659, 122
Kodama H., Sasaki M., 1984, Prog. Theor. Phys. Suppl., 78, 1
Lima J., Zanchin V., Brandenberger R. H., 1997, MNRAS, 291, L1
Linder E. V., 2003, Phys. Rev. Lett., 90, 091301
Linder E. V., 2005, Phys. Rev. D, 72, 043529
Linder E. V., Cahn R. N., 2007, Astropart. Phys., 28, 481
Ma C.-P., Bertschinger E., 1995, ApJ, 455, 7
Magnano G., Sokolowski L. M., 1994, Phys. Rev. D, 50, 5039
Mehrabi A., Malekjani M., Pace F., 2015, Ap&SS, 356, 129
Nesseris S., Perivolaropoulos L., 2005, Phys. Rev. D, 72, 123519
Nesseris S., Perivolaropoulos L., 2008, Phys. Rev. D, 77, 023504
Nesseris S., Sapone D., 2015, Int. J. Mod. Phys. D, 24, 1550045
Pace F., Batista R. C., Del Popolo A., 2014, MNRAS, 445, 648
Padmanabhan N., Xu X., Eisenstein D. J., Scalzo R., Cuesta A. J., Mehta K. T., Kazin E., 2012, MNRAS, 427, 2132
Peebles P. J. E., 1993, Principles of Physical Cosmology. Princeton Univ. Press, Princeton, NJ

Peebles P., Ratra B., 2003, Rev. Mod. Phys., 75, 559
Percival W. J. et al., 2004, MNRAS, 353, 1201
Percival W. J. et al., 2007, ApJ, 657, 645
Perlmutter S. et al., 1997, ApJ, 483, 565
Perlmutter S. et al., 1998, Nature, 391, 51
Perlmutter S. et al., 1999, ApJ, 517, 565
Planck Collaboration XIII 2015, preprint (arXiv:1502.01589)
Planck Collaboration XIV 2015, preprint (arXiv:1502.01590)
Polarski D., Gannouji R., 2008, Phys. Lett. B, 660, 439
Rapetti D., Blake C., Allen S. W., Mantz A., Parkinson D., Beutler F., 2013, MNRAS, 432, 973
Reid B. A. et al., 2012, MNRAS, 426, 2719
Riess A. G. et al., 2004, ApJ, 607, 665
Sahni V., Starobinsky A. A., 2000, Int. J. Mod. Phys. D, 9, 373
Saini T. D., Raychaudhury S., Sahni V., Starobinsky A. A., 2000, Phys. Rev. Lett., 85, 1162
Samushia L., Percival W. J., Raccanelli A., 2012, MNRAS, 420, 2102
Sapone D., Majerotto E., 2012, Phys. Rev. D, 85, 123529
Schmidt H.-J., 1990, Astron. Nachr., 311, 165
Seo H.-J., Eisenstein D. J., 2005, ApJ, 633, 575
Serra P., Cooray A., Holz D. E., Melchiorri A., Pandolfi S., Sarkar D., 2009, Phys. Rev. D, 80, 121302
Shafer D. L., Huterer D., 2014, Phys. Rev. D, 89, 063510
Simon J., Verde L., Jimenez R., 2005, Phys. Rev. D, 71, 123001
Smith R. E. et al., 2003, MNRAS, 341, 1311
Song Y.-S., Percival W. J., 2009, J. Cosmol. Astropart. Phys., 0910, 004
Spergel D. et al., 2003, ApJS, 148, 175
Spergel D. et al., 2007, ApJS, 170, 377
Spergel D. N., Flauger R., Hložek R., 2015, Phys. Rev. D, 91, 023518
Steigerwald H., Bel J., Marinoni C., 2014, J. Cosmol. Astropart. Phys., 1405, 042
Sugiura N., 1978, Commun. Stat. – Theory Methods, 7, 13
Suzuki N. et al., 2012, ApJ, 746, 85
Tegmark M. et al., 2004, Phys. Rev. D, 69, 103501
Tegmark M. et al., 2006, Phys. Rev. D, 74, 123507
Tojeiro R. et al., 2012, MNRAS, 424, 2339
Weinberg S., 1989, Rev. Mod. Phys., 61, 1
Xia J.-Q., Cai Y.-F., Qiu T.-T., Zhao G.-B., Zhang X., 2008, Int. J. Mod. Phys. D, 17, 1229
Zhang W.-S. et al., 2012, Sci. China-Phys. Mech. Astron., 55, 2244

APPENDIX A: PROOF OF EQUATION (12)

We start with equations (6) and (7). The term $\frac{\delta p}{\delta\rho}$ appears in both equations but it behaves very differently in these equations. In the first equation we have

$$-3\mathcal{H}\frac{\delta p}{\delta\rho}\delta = -3\mathcal{H}c_{\rm e}\delta - 9\frac{\mathcal{H}^2}{\rm k^2}(1+{\rm w_d})({\rm c_e}-{\rm c_a})\theta, \tag{A1}$$

and on sub-horizon scale we can neglect the latter term ($k^2 \gg \mathcal{H}^2$), but in equation (7) we have

$$k^2\frac{\delta p}{\delta\rho}\delta = k^2 c_{\rm e}\delta + 3\mathcal{H}(1+{\rm w_d})({\rm c_e}-{\rm c_a})\theta, \tag{A2}$$

where the latter term cannot be neglected. Differentiating equation (6) with respect to conformal time we have

$$\begin{aligned}\delta'' &+ w_{\rm d}'\theta + (1+w_{\rm d})\theta' + 3\mathcal{H}'c_{\rm e}\delta \\ &+ 3\mathcal{H}c_{\rm e}\delta' - 3\mathcal{H}'{\rm w_d}\delta - 3\mathcal{H}{\rm w}_{\rm d}'\delta \\ &- 3\mathcal{H}w_{\rm d}\delta' = 3w_{\rm d}'\phi' + 3(1+w_{\rm d})\phi''\end{aligned} \tag{A3}$$

Now from equation (7)

$$\begin{aligned}\theta' &= -\mathcal{H}(1-3w_{\rm d})\theta - \frac{w_{\rm d}'}{1+w_{\rm d}}\theta \\ &\quad + k^2\frac{c_{\rm e}\delta}{1+w_{\rm d}} + 3\mathcal{H}(c_{\rm e}-c_{\rm a})\theta + k^2\phi\end{aligned} \tag{A4}$$

and from equation (6)

$$\theta = 3\phi' - \frac{\delta'}{1+w_{\rm d}} - \frac{3\mathcal{H}c_{\rm e}\delta}{1+w_{\rm d}} + \frac{3\mathcal{H}w_{\rm d}\delta}{1+w_{\rm d}}. \tag{A5}$$

Substituting equations (A4) and (A5) into equation (A3), we have a second-order equation governing the evolution of DE. Changing the independent variable to the scale factor, the coefficients in equations (12) can be retrieved. On the other hand if we consider $\frac{\delta p}{\delta\rho} = c_{\rm e}$ and ignore the second term in equation (A2), we find

$$\begin{aligned}A_{\rm d} &= \frac{1}{a}\left[2 + \frac{\mathcal{H}'}{\mathcal{H}^2} + 3c_{\rm e} - 6w_{\rm d}\right], \\ B_{\rm d} &= \frac{1}{a^2}\left[3\,(c_{\rm e}-w_{\rm d})\,(1 + \frac{\mathcal{H}'}{\mathcal{H}^2} - 3w_{\rm d}) + \frac{k^2}{\mathcal{H}^2}c_{\rm e} - 3a\frac{{\rm d}w_{\rm d}}{{\rm d}a}\right], \\ S_{\rm d} &= (1+w_{\rm d})\left[3\frac{{\rm d}^2\phi}{{\rm d}a^2} + \frac{3}{a}\left(2 + \frac{\mathcal{H}'}{\mathcal{H}^2} - 3w_{\rm d}\right)\frac{{\rm d}\phi}{{\rm d}a}\right. \\ &\quad \left. - \frac{k^2}{a^2\mathcal{H}^2}\phi + \frac{3}{1+w_{\rm d}}\frac{{\rm d}\phi}{{\rm d}a}\frac{{\rm d}w_{\rm d}}{{\rm d}a}\right],\end{aligned}$$

which coincide with the values in Abramo et al. (2009) for $w_{\rm d} = $ const and $\frac{\mathcal{H}'}{\mathcal{H}^2} = -\frac{1}{2}$(matter dominated). We notice that for $w_{\rm d} = c_{\rm e} = c_{\rm a} = 0$ the coefficients for matter density contrast are recovered.

APPENDIX B: POISSON EQUATION

On sub-horizon scales, the basic equation describing the evolution of linear matter fluctuations is

$$\ddot{\delta}_{\rm m} + 2H(t)\dot{\delta}_{\rm m} + \frac{k^2}{a^2}\phi = 0. \tag{B1}$$

In this context the Poisson equation in the Fourier space is written as (Lima, Zanchin & Brandenberger 1997)

$$k^2\phi = -4\pi G a^2(\delta\rho + 3\delta p). \tag{B2}$$

where $\delta\rho = \delta\rho_{\rm m} + \delta\rho_{\rm d}$ and $\delta p = \delta p_{\rm m} + \delta p_{\rm d}$. Now using $\delta p_{\rm m} = 0$, $\delta p_{\rm d} = c_{\rm e}\delta\rho_{\rm d}$, $\delta\rho_{\rm m} = \rho_{\rm m}\delta_{\rm m}$, $\delta\rho_{\rm d} = \rho_{\rm d}\delta_{\rm d}$, and inserting the above quantities into equation (B2), we arrive to

$$-\frac{k^2}{a^2}\phi = 4\pi G[\rho_{\rm m}\delta_{\rm m} + (1+3c_{\rm e})\rho_{\rm d}\delta_{\rm d}], \tag{B3}$$

or

$$-\frac{k^2}{a^2}\phi = \frac{3}{2}H^2[\Omega_{\rm m}\delta_{\rm m} + (1+3c_{\rm e})\Omega_{\rm d}\delta_{\rm d}]. \tag{B4}$$

Utilizing the above equations it is easy to check that

$$\ddot{\delta}_{\rm m} + 2H(t)\dot{\delta}_{\rm m} = \frac{3H^2}{2}\left[\Omega_{\rm m}\delta_{\rm m} + \Omega_{\rm d}\delta_{\rm d}(1+3c_{\rm e})\right]. \tag{B5}$$

Obviously for $c_{\rm e} = w_{\rm d} = $ const, the latter equation reduces to that of Abramo et al. (2009) and Mehrabi et al. (2015). Changing the variables from t to a we finally obtain equation (39).

This paper has been typeset from a TEX/LATEX file prepared by the author.